

CONVEX ENVIRONMENTAL CONTOURS FOR NON-STATIONARY PROCESSES

ÅSMUND HAUSKEN SANDE*

ABSTRACT. Environmental contours are frequently used either as a tool in early design of marine structures or as means for circumventing expensive long-term response calculations. Here, we consider convex contours based on the assumption that all failure sets are convex. We provide a rigorous foundation for the existence of such contours when the underlying environmental factors are modelled by general, possibly non-stationary, processes. This constitutes a generalisation of existing theory and is done to properly account for empirically observed increases in extreme ocean states.

Two definitions are proposed, based respectively on averages or quantiles of failure times, along with minimal conditions on the environmental processes to guarantee existence. In order to illustrate these methods we give two examples, including an empirical study containing a method for constructing contours based on the presented theory.

Key words and phrases: Environmental Contours, Hitting Times, Structural Reliability

1. INTRODUCTION

Environmental contours are frequently used in early design of marine structures. The goal of these contours is to provide a summary statistic of extreme wave-states in order to give an alternative to the often expensive computation of structural response and, by extension, reliability. In fact, it is often the case that these contours are applied to solve the inverse problem: for a given sea-state model, which response functions allow for a predefined reliability to be met. By solving this inverse problem contours impose restrictions on which designs are permissible.

A large variety of methods for constructing environmental contours exist, for a summary and comparison of different techniques we refer to [13] and [3]. A common thread through these methods is the modelling of environmental conditions as a piecewise constant process with independent and identically distributed values in each interval. This is coupled with the property that any failure set \mathcal{F} not intersecting with the contour \mathcal{B} has at most a given probability p_e of occurring in each interval. This gives a bound on the short term failure probability and thus allows a conservative estimate of long-term response.

Arguably, the most popular of these methods is the inverse first order reliability method (IFORM) developed in [16]. This method first establishes a wave-state

* DEPARTMENT OF MATHEMATICS, UNIVERSITY OF OSLO, MOLTKE MOES VEI 35, P.O. BOX 1053 BLINDERN, 0316 OSLO, NORWAY.

E-mail address: aasmunhs@math.uio.no.

distribution which induces a Rosenblatt transformation (see [12]) of the density. All failure sets are then implicitly assumed to be convex in the transformed space, implying that the contour in the original space can be constructed by applying the inverse Rosenblatt transformation to a circle.

Some theoretical weaknesses of IFORM was discussed in [6] where they developed a definition of convex environmental contours by assuming the failure set to be convex in the original space. This approach has several advantages, such as the easy inclusion of omission factors and a more amenable interpretation of the convexity assumption compared to IFORM. Several improvements and possible modifications to this method has been made in e.g. [1], [5], and [7].

However, this method still relies on a stationary model with independent piecewise constant values. This causes issues when taken together with the evidence of increasingly extreme wave states as detailed in [15],[14], and [8], which would imply a significant non-stationarity in the wave heights. Several articles such as [14] and [6] adjust the wave-state distributions to correct for this increase in wave heights, but the models are still stationary which keeps them from fully representing the changing behaviour of the environmental processes involved. A closer view on the differences between such strategies and the methods to be presented in this paper will be given in Section 5.

It's also worth mentioning is the works of e.g. [9] and [10] which consider stationary processes with a varying degree of autodependence. These articles allow for more general behaviours of the underlying environmental processes, but do not address the issue of long-term trends.

The goal of this article is to present a rigorous definition of environmental contours with a broad class of possible models, including non-stationary ones, for the underlying environmental factors. In doing so we will give minimal conditions for relevant functions to be well defined in addition to existence of the contours themselves. Results presented in this article will be a generalisation of the theory discussed in [6],[7], and [5] which are based on the assumption of failure sets being convex in the original parameter space. As such we will in Section 2 give a brief overview of the main results from these papers for so to generalize the setting in Section 3. We will here propose two different ways of defining convex environmental contours based on either averages or quantiles of exceedance times. In Section 4 and 5 we present two examples of applications of the theory which highlight some of the differences between classical approaches and the more flexible methods allowed by the theory presented in this article. As a part of the final example we also present a method for computing these contours in a practical sense.

2. CONVEX CONTOURS

A *convex environmental contour* is the boundary of a compact convex set $\mathcal{B} \subset \mathbb{R}^d$, denoted $\partial\mathcal{B}$, defined with respect to a collection of d environmental processes. For example, these processes are sometimes taken to be the pair $V = (P, H)$ for $d = 2$ where P is the zero up-crossing wave period and H the significant wave height of a particular location of interest.

We will in this section follow the construction described in e.g. [7] and [5] and assume that the distribution of V_t is constant and absolutely continuous with respect to the Lebesgue measure on \mathbb{R}^d . Furthermore, the process is assumed to be path-wise constant over periods of a set length of Δt , and most importantly we make the assumption that values of V are independent between these different periods. One could equivalently consider $V_t = W_{\lfloor t/\Delta t \rfloor}$ where $\lfloor \cdot \rfloor$ denotes the floor function and with $\{W_n\}_{n=0}^\infty$ defined as a sequence of independent and identically distributed (i.i.d.) random variables with a distribution equal to that of V . As such we will refer to this type of model as an *i.i.d. model* throughout this article.

We are also considering a failure region $\mathcal{F} \subset \mathbb{R}^d$, this set is often unknown in the early design phases where environmental contours are used. In order to handle an unknown \mathcal{F} we assume that \mathcal{F} belongs to $\mathcal{E}(\mathcal{B})$, the class of all convex sets such that $\mathcal{F} \cap \mathcal{B} \subseteq \partial\mathcal{B}$. Based on this we may define the *exceedance probability* by

$$P_e(\mathcal{B}, \mathcal{E}) = \sup_{\mathcal{F} \in \mathcal{E}(\mathcal{B})} \mathbb{P}(V \in \mathcal{F}). \quad (2.1)$$

and impose the constraint of

$$P_e(\mathcal{B}, \mathcal{E}) \leq p_e, \quad (2.2)$$

where p_e is some given target exceedance probability.

When dealing with convexity we will need the concept of hyperplanes. We will denote by $\langle \cdot, \cdot \rangle$ the canonical inner product on \mathbb{R}^d and by $\|\cdot\|$ the euclidean norm, with this we also define the unit sphere on \mathbb{R}^d by $S^{d-1} = \{v \in \mathbb{R}^d : \|v\| = 1\}$. The hyperplane indexed by the threshold $c \in \mathbb{R}$ and the unit vector $u \in S^{d-1}$ is then defined as

$$\Pi(u, c) = \{v \in \mathbb{R}^d : \langle u, v \rangle = c\}. \quad (2.3)$$

We further define the half-spaces

$$\begin{aligned} \Pi^-(u, c) &= \{v \in \mathbb{R}^d : \langle u, v \rangle \leq c\}, \\ \Pi^+(u, c) &= \{v \in \mathbb{R}^d : \langle u, v \rangle \geq c\}, \end{aligned} \quad (2.4)$$

which allow us to present an important well-known result about separating hyperplanes.

Proposition 2.1. *For any two convex sets \mathcal{B} and \mathcal{F} in \mathbb{R}^d such that $\mathcal{B} \cap \mathcal{F} \subseteq \partial\mathcal{B}$ there exists some $u \in S^{d-1}$, $c \in \mathbb{R}$ such that $\mathcal{B} \subseteq \Pi^-(u, c)$ and $\mathcal{F} \subseteq \Pi^+(u, c)$.*

This result, as shown in [7] for $d = 2$, implies that we can separate a convex set \mathcal{B} and any $\mathcal{F} \in \mathcal{E}(\mathcal{B})$. In particular, we can reconstruct any compact and convex \mathcal{B} as the intersection of all these half-spaces. If we define

$$B(\mathcal{B}, u) = \sup\{\langle u, v \rangle : v \in \mathcal{B}\}, \quad (2.5)$$

we get that \mathcal{B} can be represented as

$$\mathcal{B} = \bigcap_{u \in S^{d-1}} \Pi^-(u, B(\mathcal{B}, u)). \quad (2.6)$$

It is further shown that these hyperplanes that define \mathcal{B} serve as maximal elements for computing the exceedance probability, yielding

$$P_e(\mathcal{B}, \mathcal{E}) = \sup_{u \in S^{d-1}} \mathbb{P}(V \in \Pi^+(u, B(\mathcal{B}, u))). \quad (2.7)$$

Based on this, if we have an environmental contour $\partial\mathcal{B}$ such that \mathcal{B} is convex and compact we will call $\partial\mathcal{B}$ a *valid contour in the exceedance probability sense* if $P_e(\mathcal{B}, \mathcal{E}) \leq p_e$, and a *proper contour in the exceedance probability sense* if, for all $u \in S^{d-1}$, $\mathbb{P}(V \in \Pi^+(u, B(\mathcal{B}, u))) = p_e$. The goal is then to construct the smallest convex and compact set with a valid or, ideally, proper contour.

If we then define

$$C_e(u) = \inf\{C : \mathbb{P}(\langle u, V \rangle > C) = p_e\}, \quad (2.8)$$

and if $B(\mathcal{B}, u) \geq C_e(u)$ for all $u \in S^{d-1}$ we get $P_e(\mathcal{B}, \mathcal{E}) \leq p_e$, making $\partial\mathcal{B}$ a valid contour. In particular if there exists any convex \mathcal{B} such that $B(\mathcal{B}, u) = C_e(u)$ then this construction guarantees that \mathcal{B} is the minimal contour satisfying $P_e(\mathcal{B}, \mathcal{E}) = p_e$. Lastly, if this is the case, then

$$\mathcal{B} = \bigcap_{u \in S^{d-1}} \Pi^-(u, C_e(u)), \quad (2.9)$$

gives an explicit construction of this optimal proper contour.

In the following sections we will need the concept of the first hitting time of a set $\mathcal{F} \subseteq \mathbb{R}^d$, defined by

$$\tau_{\mathcal{F}} = \inf\{t : V_t \in \mathcal{F}\} \quad (2.10)$$

For our i.i.d. model we can easily associate our target exceedance probability with a target return period. We can note that by our assumption of independence between the W_n 's that the exceedance time, $\tau_{\mathcal{F}}$, for any valid $\partial\mathcal{B}$ and $\mathcal{F} \in \mathcal{E}(\mathcal{B})$ is geometrically distributed with a mean of at least $\Delta t/p_e$. This implies that when we are ensuring that $P_e(\mathcal{B}, \mathcal{E}) \leq p_e$ we are equivalently ensuring that $\mathbb{E}[\tau_{\mathcal{F}}] \geq t_r$ for some target return period $t_r = \Delta t/p_e$. Similar arguments would allow us to compare $P_e(\mathcal{B}, \mathcal{E})$ with quantiles of the distribution of $\tau_{\mathcal{F}}$. Both the mean and quantiles of $\tau_{\mathcal{F}}$ are more amenable to generalisation than exceedance probabilities and will be used in the upcoming sections.

3. ENVIRONMENTAL CONTOURS FOR GENERAL PROCESSES

We now aim to extend the concepts introduced in the previous section to a more general context. We no longer assume V to be stationary and instead consider it to be a progressively measurable process taking values in \mathbb{R}^d . We also need the process to satisfy certain regularity conditions in order to ensure that (3.9), which will be introduced later, is measurable. For this purpose one may assume, for instance, càdlàg paths.

We will also still consider an unknown failure region $\mathcal{F} \in \mathcal{E}(\mathcal{B})$ where $\mathcal{E}(\mathcal{B})$ is the collection of all convex sets \mathcal{F} such that $\mathcal{F} \cap \mathcal{B} \subseteq \partial\mathcal{B}$. This will similarly allow the use of half-spaces to control the exceedance time.

Since we no longer assume a stationary distribution, we will introduce two ways of replacing equation (2.1). A common substitute for the exceedance probability, used

explicitly in works such as [9] and [10], is to use the average failure time, commonly referred to as a *return period*. As such, we start by defining the *return period of \mathcal{B}* by

$$T_r(\mathcal{B}) = \inf_{\mathcal{F} \in \mathcal{E}(\mathcal{B})} \mathbb{E}[\tau_{\mathcal{F}}]. \quad (3.1)$$

Remark 3.1. *Since V is now possibly non-stationary the concept of a long-term average return period is no longer meaningful. However, for the sake of consistency, we shall still refer to these average exceedance times as return periods.*

In some cases there may be yearly trends present which, if persisting indefinitely, may cause the process to drift over time. In such cases there could be a positive probability that the process never exits certain sets which contrasts with the stationary case where every set of positive measure (w.r.t. the law of V) is eventually hit. While the exceedance time might have a positive probability of not occurring, thereby making the return period infinite, there could still be a high chance of it occurring in finite time. In order to account for such behaviour we want a more flexible version of (3.1). As such we define the *survival probability of \mathcal{B}* by

$$Q_s(\mathcal{B}) = \inf_{\mathcal{F} \in \mathcal{E}(\mathcal{B})} \mathbb{P}(\tau_{\mathcal{F}} > t_s), \quad (3.2)$$

for a given *survival time* $t_s > 0$.

Like with equation (2.2) we will construct our contour based on these two definitions. In our case we will consider two separate possible restrictions, the first one is based on return periods with

$$T_r(\mathcal{B}) \geq t_r \quad (3.3)$$

for some target return period $t_r > 0$. If this holds then for any $\mathcal{F} \in \mathcal{E}(\mathcal{B})$ it will take on average at least a time of t_r to enter \mathcal{F} . Note that under the constraints of an i.i.d model, equation (3.3) is equivalent to equation (2.2) for $t_r = \Delta t/p_e$.

The alternative restriction corresponding to the survival probability is defined as

$$Q_s(\mathcal{B}) \geq q_s \quad (3.4)$$

for a given minimal survival probability $1 > q_s > 0$. If this condition holds, then for any $\mathcal{F} \in \mathcal{E}(\mathcal{B})$, it is guaranteed that with a probability of at least q_s , the process V will take at least t_s amount of time before hitting \mathcal{F} . Note that under the constraints of an i.i.d model, τ has a geometric distribution which means equation (3.4) is equivalent to equation (2.2) if e.g. $t_s = \Delta t/p_e$ and $q_s = (1 - p_e)^{1/p_e}$. In particular, for low exceedance probabilities, we have that $q_s \approx 1/e \approx 37\%$.

With these possible constraints established we now have two new ways of defining our environmental contours, either by (3.3) or (3.4). As noted, both of these serve as generalizations of the restriction of equation (2.2). Analogously to the previous section we will refer to a contour $\partial\mathcal{B}$ such that \mathcal{B} is convex and compact as *valid in the return period sense* if $T_r(\mathcal{B}) \geq t_r$ and *valid in the quantile sense* if $Q_s(\mathcal{B}) \geq q_s$. Likewise, we call $\partial\mathcal{B}$ *proper in the return period sense* if $\mathbb{E}[\tau_{\Pi^+(u, B(\mathcal{B}, u))}] = t_r$ for all $u \in S^{d-1}$ and *proper in the quantile sense* if $\mathbb{P}(\tau_{\Pi^+(u, B(\mathcal{B}, u))} > t_s) = q_s$ for all $u \in S^{d-1}$. In order to justify the definitions of proper contours we proceed analogously to [7] by the following result.

Proposition 3.2. *Let $\mathcal{B} \subset \mathbb{R}^d$ be a compact and convex set, we then have*

$$Q_s(\mathcal{B}) = \inf_{u \in S^{d-1}} \mathbb{P}(\tau_{\Pi^+(u, B(\mathcal{B}, u))} > t_s),$$

$$T_r(\mathcal{B}) = \inf_{u \in S^{d-1}} \mathbb{E}[\tau_{\Pi^+(u, B(\mathcal{B}, u))}].$$

Proof. We first note that by Proposition 2.1 we have for any $\mathcal{F} \in \mathcal{E}(\mathcal{B})$ that $\mathcal{F} \subseteq \Pi^+(u, c)$ and $\mathcal{B} \subseteq \Pi^-(u, c)$ for some $u \in S^{d-1}$, $c \in \mathbb{R}$. This yields $B(\mathcal{B}, u) \leq c$, which implies $\Pi^+(u, c) \subseteq \Pi^+(u, B(\mathcal{B}, u))$. Since $\mathcal{F} \subseteq \Pi^+(u, B(\mathcal{B}, u))$ we then have $\tau_{\mathcal{F}} \geq \tau_{\Pi^+(u, B(\mathcal{B}, u))}$ which further implies that

$$\mathbb{P}(\tau_{\mathcal{F}} > t_r) \geq \mathbb{P}(\tau_{\Pi^+(u, B(\mathcal{B}, u))} > t_r),$$

$$\mathbb{E}[\tau_{\mathcal{F}}] \geq \mathbb{E}[\tau_{\Pi^+(u, B(\mathcal{B}, u))}].$$

This inequality yields

$$\inf_{\mathcal{F} \in \mathcal{E}(\mathcal{B})} \mathbb{P}(\tau_{\mathcal{F}} \geq t_s) \geq \inf_{u \in S^{d-1}} \mathbb{P}(\tau_{\Pi^+(u, B(\mathcal{B}, u))} > t_r),$$

$$\inf_{\mathcal{F} \in \mathcal{E}(\mathcal{B})} \mathbb{E}[\tau_{\mathcal{F}}] \geq \inf_{u \in S^{d-1}} \mathbb{E}[\tau_{\Pi^+(u, B(\mathcal{B}, u))}],$$

and the result then follows by noting that $\Pi^+(u, B(\mathcal{B}, u)) \in \mathcal{E}(\mathcal{B})$ for any $u \in S^{d-1}$. \square

With this we can introduce our analogues of C_e from equation (2.8) by

$$C_Q(u) = \inf\{b \in \mathbb{R} : \mathbb{P}(\tau_{\Pi^+(u, b)} > t_s) = q_s\}, \quad (3.5)$$

$$C_T(u) = \inf\{b \in \mathbb{R} : \mathbb{E}[\tau_{\Pi^+(u, b)}] = t_r\}. \quad (3.6)$$

In order to ensure these functions are well defined we will need the following definitions and results. For any $u \in S^{d-1}$, $b \in \mathbb{R}$ and $t \in \mathbb{R}$ with $t \geq 0$, we denote the cumulative distribution function of $\tau_{\Pi^+(u, b)}$ by

$$F_b^u(t) = \mathbb{P}(\tau_{\Pi^+(u, b)} \leq t), \quad (3.7)$$

and the average of $\tau_{\Pi^+(u, b)}$ by

$$\mathcal{T}_u(b) = \mathbb{E}[\tau_{\Pi^+(u, b)}]. \quad (3.8)$$

Finally we define

$$\phi_t^u = \sup_{s \in [0, t]} \langle V_s, u \rangle. \quad (3.9)$$

Throughout this article we will usually assume that for any $t > 0$, $b \in \mathbb{R} \cup \{\pm\infty\}$ we have

$$\mathbb{P}(\phi_t^u = b) = 0. \quad (3.10)$$

This assumption will serve as a minimum condition for our contours and other concepts to be definable. For most models, (3.10) will follow as a consequence of ϕ_t^u admitting a continuous density for every $u \in S^{d-1}$ and $t > 0$. To see the connection between these definitions we have the following result.

Lemma 3.3. *Let $u \in S^{d-1}$ and $t > 0$, we then have*

$$\mathcal{T}_u(b) = \int_0^\infty (1 - F_b^u(t)) dt.$$

Furthermore, if (3.10) holds, then

$$F_b^u(t) = \mathbb{P}(\phi_t^u \geq b).$$

Proof. The first equality is the standard tail probability expectation formula, as such we omit the proof.

As for the second equality, if $\tau_{\Pi^+(u,b)} \leq t$ then there is some point $s \leq t$ such that $V_s \in \Pi^+(u, b)$, or equivalently $\langle V_s, u \rangle \geq b$, which implies $\phi_t^u \geq b$. Similarly, if $\tau_{\Pi^+(u,b)} > t$ then no such point exists and consequently $\phi_t^u \leq b$, this conversely states that $\phi_t^u > b$ implies $\tau_{\Pi^+(u,b)} \leq t$.

Applying these implications and (3.10) we get

$$\mathbb{P}(\tau_{\Pi^+(u,b)} \leq t) \leq \mathbb{P}(\phi_t^u \geq b) = \mathbb{P}(\phi_t^u > b) \leq \mathbb{P}(\tau_{\Pi^+(u,b)} \leq t),$$

which proves the second equality. \square

With this lemma we can prove the following results which guarantee that (3.5) and (3.6) are well defined.

Theorem 3.4. *Under the assumption of (3.10) we have for any $t > 0$, $u \in S^{d-1}$ that $b \mapsto F_b^u(t)$ is monotone non-increasing and continuous with $\lim_{b \rightarrow \infty} F_b^u(t) = 0$ and $\lim_{b \rightarrow -\infty} F_b^u(t) = 1$.*

Proof. We will start by showing that F is monotone non-increasing in b . If $b \leq b'$ then $\Pi^+(u, b') \subseteq \Pi^+(u, b)$ which implies $\tau_{\Pi^+(u,b)} \leq \tau_{\Pi^+(u,b')}$, finally yielding that $F_{b'}^u(t) \leq F_b^u(t)$.

For the continuity we start by showing left-continuity of $b \mapsto F_b^u(t)$. Whenever $b_n \rightarrow b$, $b_n < b_{n+1}$ we have by set-continuity of measures and Lemma 3.3 that

$$\begin{aligned} \lim_{n \rightarrow \infty} F_{b_n}^u(t) - F_b^u(t) &= \lim_{n \rightarrow \infty} \mathbb{P}(\tau_{\Pi^+(u,b_n)} \leq t) - \mathbb{P}(\tau_{\Pi^+(u,b)} \leq t) \\ &= \mathbb{P}\left(\bigcap_n \{\tau_{\Pi^+(u,b_n)} \leq t\}\right) - \mathbb{P}(\tau_{\Pi^+(u,b)} \leq t) \\ &= \mathbb{P}(\tau_{\Pi^+(u,b_n)} \leq t \text{ for all } n) - \mathbb{P}(\tau_{\Pi^+(u,b)} \leq t) \\ &= \mathbb{P}(\phi_t^u \geq b_n \text{ for all } n) - \mathbb{P}(\phi_t^u \geq b). \end{aligned}$$

We see that $\phi_t^u \geq b_n$ for all n , is equivalent to $\phi_t^u \geq b$. This implies that the limit equals $\mathbb{P}(\phi_t^u \geq b) - \mathbb{P}(\phi_t^u \geq b) = 0$, thus proving the left-continuity of $b \mapsto F_b^u(t)$.

As for right-continuity we consider $b_n \rightarrow b$, $b_n > b_{n+1}$ and get

$$\begin{aligned}
F_b^u(t) - \lim_{n \rightarrow \infty} F_{b_n}^u(t) &= \mathbb{P}(\tau_{\Pi^+(u,b)} \leq t) - \lim_{n \rightarrow \infty} \mathbb{P}(\tau_{\Pi^+(u,b_n)} \leq t) \\
&= \mathbb{P}(\tau_{\Pi^+(u,b)} \leq t) - \mathbb{P}\left(\bigcup_n \{\tau_{\Pi^+(u,b_n)} \leq t\}\right) \\
&= \mathbb{P}(\phi_t^u \geq b) - \mathbb{P}\left(\bigcup_n \{\phi_t^u \geq b_n\}\right) \\
&= \mathbb{P}(\phi_t^u \geq b) - 1 + \mathbb{P}\left(\bigcap_n \{\phi_t^u < b_n\}\right) \\
&= \mathbb{P}(\phi_t^u > b) + \mathbb{P}(\phi_t^u < b_n \text{ for all } n) - 1
\end{aligned}$$

Similarly to before we note that $\phi_t^u < b_n$ for all n is equivalent to $\phi_t^u \leq b$. As a consequence the limit equals $\mathbb{P}(\phi_t^u \in \mathbb{R}) - 1 = 0$, which implies that $b \mapsto F_b^u(t)$ is right-continuous and therefore fully continuous.

Considering $\lim_{b \rightarrow \infty} F_b^u(t)$ we may, for any sequence $b_n \rightarrow \infty$, $b_n < b_{n+1}$, compute

$$\begin{aligned}
\lim_{n \rightarrow \infty} F_{b_n}^u(t) &= \lim_{n \rightarrow \infty} \mathbb{P}(\tau_{\Pi^+(u,b_n)} \leq t) \\
&= \lim_{n \rightarrow \infty} \mathbb{P}(\phi_t^u \geq b_n) \\
&= \mathbb{P}(\phi_t^u \geq b_n \text{ for all } n) \\
&= \mathbb{P}(\phi_t^u = \infty) \\
&= 0.
\end{aligned}$$

And lastly, for $\lim_{b \rightarrow -\infty} F_b^u(t)$ we get, for any sequence $b_n \rightarrow -\infty$, $b_n > b_{n+1}$, that

$$\begin{aligned}
\lim_{n \rightarrow \infty} F_{b_n}^u(t) &= \lim_{n \rightarrow \infty} \mathbb{P}(\tau_{\Pi^+(u,b_n)} \leq t) \\
&= 1 - \lim_{n \rightarrow \infty} \mathbb{P}(\tau_{\Pi^+(u,b_n)} > t) \\
&= 1 - \lim_{n \rightarrow \infty} \mathbb{P}(\phi_t^u \leq b_n) \\
&= 1 - \mathbb{P}(\phi_t^u \leq b_n \text{ for all } n) \\
&= 1 - \mathbb{P}(\phi_t^u = -\infty) \\
&= 1,
\end{aligned}$$

which completes the proof. \square

Remark 3.5. *Continuity of $b \mapsto F_b^u(t)$ and $\lim_{b \rightarrow \infty} F_b^u(t) = 0$ for all $u \in S^{d-1}$ is equivalent to the assumption of (3.10), making it a necessary and sufficient condition for Theorem 3.4.*

This theorem implies that $b \mapsto 1 - F_b^u(t_s) = \mathbb{P}(\tau_{\Pi^+(u,b)} > t_s)$ spans $(0, 1)$ which implies that C_Q is well defined for any $q_s \in (0, 1)$. To ensure that C_T is also well defined, we have the following result.

Proposition 3.6. *Assume that (3.10) holds and that for any $u \in S^{d-1}$ there is some $b_u^* \in \mathbb{R} \cup \{\infty\}$ such that $\mathcal{T}_u(b) < \infty$ for all $b \in (-\infty, b_u^*)$ with $\mathcal{T}_u(b) = \infty$ for all $b \geq b_u^*$. We then have that $\mathcal{T}_u(\cdot)$ is continuous and monotone non-decreasing on $(-\infty, b_u^*)$ with $\lim_{b \rightarrow -\infty} \mathcal{T}_u(b) = 0$ and $\lim_{b \rightarrow b_u^*} \mathcal{T}_u(b) = \infty$.*

Proof. We start with monotonicity. If $b \leq b'$ then $\Pi^+(u, b') \subseteq \Pi^+(u, b)$ which means $\tau_{\Pi^+(u, b)} \leq \tau_{\Pi^+(u, b')}$, implying $\mathcal{T}_u(b) \leq \mathcal{T}_u(b')$.

As for continuity, if $b_n \rightarrow b \in (-\infty, b_u^*)$ there exists some $\epsilon > 0$ and some $N \in \mathbb{N}$ such that $b_n < b + \epsilon$ for all $n > N$ with $b + \epsilon \in (-\infty, b_u^*)$. This means that $1 - F_{b_n}^u(t) \leq 1 - F_{b+\epsilon}^u(t)$ for all $n > N$ and $\mathcal{T}_u(b + \epsilon) = \int_0^\infty (1 - F_{b+\epsilon}^u(t)) dt < \infty$. We then get by continuity of $b \mapsto F_b^u(t)$ and the dominated convergence theorem that

$$\begin{aligned} \lim_{n \rightarrow \infty} \mathcal{T}_u(b_n) &= \lim_{n \rightarrow \infty} \int_0^\infty (1 - F_{b_n}^u(t)) dt \\ &= \int_0^\infty \left(1 - \lim_{n \rightarrow \infty} F_{b_n}^u(t)\right) dt \\ &= \int_0^\infty (1 - F_b^u(t)) dt \\ &= \mathcal{T}_u(b). \end{aligned}$$

Similarly, for $b_n \rightarrow -\infty$, we have some N and $b' \in (-\infty, b_u^*)$ such that $b_n < b'$ for all $n > N$. Since $1 - F_{b_n}^u(t) \leq 1 - F_{b'}^u(t)$ for $n > N$ we get by the dominated convergence theorem, along with $\lim_{b \rightarrow -\infty} F_b^u(t) = 1$, that

$$\begin{aligned} \lim_{b \rightarrow -\infty} \mathcal{T}_u(b) &= \lim_{b \rightarrow -\infty} \int_0^\infty (1 - F_b^u(t)) dt \\ &= \int_0^\infty \left(1 - \lim_{b \rightarrow -\infty} F_b^u(t)\right) dt \\ &= \int_0^\infty 0 dt \\ &= 0. \end{aligned}$$

Lastly, for $b_n \rightarrow b_u^* < \infty$, we start with right limits and assume $b_n \geq b_{n+1}$ for all n with $b_n \rightarrow b_u^* < \infty$. Since $b_n \geq b_u^*$ we have $\mathcal{T}_u(b_n) = \infty$ for all n which yields $\mathcal{T}_u(b_n) \rightarrow \infty = \mathcal{T}_u(b)$.

We then consider the left limit case, i.e. $b_n \leq b_{n+1}$ for all n , $b_n \rightarrow b_u^*$. We then have that $\{1 - F_{b_n}^u\}_{n=1}^\infty$ is a monotone increasing sequence of non-negative functions,

as such we get by the monotone convergence theorem that

$$\begin{aligned}
\lim_{b \rightarrow b_u^*} \mathcal{T}_u(b) &= \lim_{b \rightarrow b_u^*} \int_0^\infty (1 - F_b^u(t)) dt \\
&= \int_0^\infty \left(1 - \lim_{b \rightarrow b_u^*} F_b^u(t) \right) dt \\
&= \int_0^\infty (1 - F_{b_u^*}^u(t)) dt \\
&= \mathcal{T}_u(b_u^*) \\
&= \infty.
\end{aligned}$$

The same computations would hold if $b_u^* = \infty$ by considering $F_\infty^u = 0$, which completes the proof. \square

With this result we see that, under the given assumptions, $\mathcal{T}_u(\cdot)$ spans the whole of $(0, \infty)$ so C_T is well defined for any $t_r \in (0, \infty)$.

With this both our analogues of C_e from equation (2.8) are well defined. Similarly to [7], we can use these functions to guarantee certain properties of our contours.

Proposition 3.7. *Fix some $t_s \in (0, \infty)$, $q_s \in (0, 1)$ such that $C_Q(u)$ is well defined for all $u \in S^{d-1}$. We then have that $Q_s(\mathcal{B}) \geq p_s$ is equivalent to*

$$B(\mathcal{B}, u) \geq C_Q(u) \text{ for all } u \in S^{d-1}.$$

Furthermore, if we fix some $t_r > 0$ such that C_T is well defined, then $T_r(\mathcal{B}) \geq t_r$ is equivalent to

$$B(\mathcal{B}, u) \geq C_T(u) \text{ for all } u \in S^{d-1}.$$

Proof. We start by assuming that $B(\mathcal{B}, u) \geq C_Q(u)$ for all $u \in S^{d-1}$ and get

$$Q_s(\mathcal{B}) = \inf_{u \in S^{d-1}} \left\{ \mathbb{P}(\tau_{\Pi^+(u, B(\mathcal{B}, u))} > t_s) \right\} \geq \inf_{u \in S^{d-1}} \left\{ \mathbb{P}(\tau_{\Pi^+(u, C_Q(u))} > t_s) \right\} = q_s.$$

Conversely, if $B(\mathcal{B}, u') < C_Q(u')$ for some $u' \in S^{d-1}$ then by the definition of C_Q we must have $\mathbb{P}(\tau_{\Pi^+(u', B(u'))} > t_s) < p_s$. This implies

$$Q_s(\mathcal{B}) = \inf_{u \in S^{d-1}} \left\{ \mathbb{P}(\tau_{\Pi^+(u, B(\mathcal{B}, u))} > t_s) \right\} \leq \mathbb{P}(\tau_{\Pi^+(u', B(\mathcal{B}, u'))} > t_s) < q_s.$$

An identical argument proves the statement about T_r which completes the proof. \square

Recall that we can write

$$\mathcal{B} = \bigcap_{u \in S^{d-1}} \Pi^-(u, B(\mathcal{B}, u)), \quad (3.11)$$

so if there exists some \mathcal{B} with $B(\mathcal{B}, u) = C(u)$ for all $u \in S^{d-1}$, then we can immediately construct \mathcal{B} by

$$\mathcal{B} = \bigcap_{u \in S^{d-1}} \Pi^-(u, C(u)), \quad (3.12)$$

for e.g. $C = C_e$, C_T or C_Q . In [7] it is shown for an i.i.d. model of V that, under some conditions, $B(\mathcal{B}, u) = C_e(u)$ is equivalent to $\partial\mathcal{B}$ being proper in the exceedance probability sense. This implies that all proper contours are constructable in the same

fashion as (3.12). An analogous result also holds in our setting for C_Q or C_T under some light assumptions.

Proposition 3.8. *For any $u \in S^{d-1}$, $t \in (0, \infty)$, define the set $\mathcal{U}_t^u = \{b : F_b^u(t) \in (0, 1)\}$ and assume that ϕ_t^u admits a density, denoted by f_t^u , satisfying $f_t^u(b) > 0$ for all $b \in \mathcal{U}_t^u$. Note that this last requirement is equivalent to the support of f_t^u being a connected interval.*

We have that $b \mapsto F_b^u(t)$ is monotone decreasing on \mathcal{U}_t^u . Furthermore, if there exists some proper contour $\partial\mathcal{B}$ in the quantile sense, i.e. $\mathbb{P}(\tau_{\Pi^+(u, B(\mathcal{B}, u))} > t_s) = q_s$ for all $u \in S^{d-1}$, then $B(\mathcal{B}, \cdot) = C_Q$ and therefore

$$\mathcal{B} = \bigcap_{u \in S^{d-1}} \Pi^-(u, C_Q(u)).$$

Proof. Since ϕ_t^u admits a density we have that $\mathbb{P}(\phi_t^u = b) = 0$ for all $b \in \mathbb{R}$ which implies by Theorem 3.4 that $b \mapsto F_b^u(t)$ is continuous and monotone non-increasing, in particular we note that \mathcal{U}_t^u is open for all $u \in S^{d-1}$, $t \in (0, \infty)$.

We first aim to prove that $b \mapsto F_b^u(t)$ is monotone decreasing on \mathcal{U}_t^u . To see this we consider $b \in \mathcal{U}_t^u$ and $b' \in \mathbb{R}$ such that $b < b'$. Since \mathcal{U}_t^u is open we can find an $\epsilon > 0$ such that $(b, b + \epsilon) \subseteq \mathcal{U}_t^u$ and $b + \epsilon < b'$. Additionally, we have

$$\mathbb{P}(\phi_t^u \in (b, b + \epsilon)) = \int_b^{b+\epsilon} f_t^u(x) dx > 0.$$

Combining this with Lemma 3.3 then yields

$$\begin{aligned} F_b^u(t) - F_{b'}^u(t) &= \mathbb{P}(\tau_{\Pi^+(u, b)} \leq t) - \mathbb{P}(\tau_{\Pi^+(u, b')} \leq t) \\ &= \mathbb{P}(\phi_t^u > b) - \mathbb{P}(\phi_t^u \geq b') \\ &= \mathbb{P}(\phi_t^u \in (b, b')) \\ &\geq \mathbb{P}(\phi_t^u \in (b, b + \epsilon)) \\ &> 0, \end{aligned}$$

which implies $F_b^u(t) > F_{b'}^u(t)$.

Consider then some proper contour $\partial\mathcal{B}$, and assume, for contradiction, that we have $B(\mathcal{B}, u) > C_Q(u)$ for some $u \in S^{d-1}$. Since, by definition, $C_Q(u) \in \mathcal{U}_{t_s}^u$ we must also have $F_{C(u)}^u(t_s) > F_{B(\mathcal{B}, u)}^u(t_s)$ which yields

$$\begin{aligned} \mathbb{P}(\tau_{\Pi^+(u, B(\mathcal{B}, u))} > t_s) &= 1 - F_{B(\mathcal{B}, u)}^u(t_s) \\ &> 1 - F_{C_Q(u)}^u(t_s) \\ &= \mathbb{P}(\tau_{\Pi^+(u, C_Q(u))} > t_s) \\ &= q_s. \end{aligned}$$

This contradicts the fact that $\partial\mathcal{B}$ is a proper contour and we must therefore have $B(\mathcal{B}, u) = C_Q(u)$ for all $u \in S^{d-1}$. \square

We can also extend this result to proper contours in the return period sense.

Proposition 3.9. *Fix some t_r such that $C_T(u)$ is defined for all $u \in S^{d-1}$ and let the conditions of Proposition 3.8 hold. We also assume that $\tau_{\Pi^+(u, C(u))}$ is non-deterministic in the sense that $\mathbb{P}(\tau_{\Pi^+(u, C(u))} = t_r) < 1$.*

Under these conditions, if there exists some proper contour $\partial\mathcal{B}$ in the return period sense, i.e. $\mathbb{E}[\tau_{\Pi^+(u, B(\mathcal{B}, u))}] = t_r$ for all $u \in S^{d-1}$, then $B(\mathcal{B}, \cdot) = C_T$ and

$$\mathcal{B} = \bigcap_{u \in S^{d-1}} \Pi^-(u, C_T(u)).$$

Proof. Consider the proper contour $\partial\mathcal{B}$ and assume for contradiction that $B(\mathcal{B}, u) > C_T(u)$ for some $u \in S^{d-1}$. We then have that since $\mathcal{T}_u(B(\mathcal{B}, u)) = \mathcal{T}_u(C_T(u))$ then

$$\begin{aligned} 0 &= \mathcal{T}_u(C(u)) - \mathcal{T}_u(B(\mathcal{B}, u)) \\ &= \int_0^\infty (1 - F_{C_T(u)}^u(t)) dt - \int_0^\infty (1 - F_{B(\mathcal{B}, u)}^u(t)) dt \\ &= \int_0^\infty (F_{B(\mathcal{B}, u)}^u(t) - F_{C_T(u)}^u(t)) dt. \end{aligned}$$

Since $F_{B(\mathcal{B}, u)}^u(t) - F_{C_T(u)}^u(t) \geq 0$ this equality implies $F_{B(\mathcal{B}, u)}^u(t) = F_{C_T(u)}^u(t)$ for almost all $t \in [0, \infty)$. However, $b \mapsto F_b^u(t)$ is monotone decreasing on \mathcal{U}_t^u , so we must have $C_T(u) \notin \mathcal{U}_t^u$, implying $F_{C_T(u)}^u(t) \in \{0, 1\}$, for almost all $t \in [0, \infty)$. Furthermore, since $t \mapsto F_b^u(t)$ is monotone non-decreasing $F_{C_T(u)}^u(t)$ either equals $\mathbf{1}(t < s)$ or $\mathbf{1}(t \leq s)$ for some $s \in [0, \infty)$, where $\mathbf{1}$ denotes the indicator function. In fact, since $\int_0^\infty (1 - F_{C_T(u)}^u(t)) dt = t_r$ we get $F_{C_T(u)}^u(t) = \mathbf{1}(t < t_r)$ or $\mathbf{1}(t \leq t_r)$. From this we see that $\mathbb{P}(\tau_{\Pi^+(u, C(u))} = t_r) = 1$ which contradicts our assumption that $\tau_{\Pi^+(u, C(u))}$ is non-deterministic, thereby implying $B(\mathcal{B}, u) = C_T(u)$ for all $u \in S^{d-1}$. \square

These results shows us that any proper contour, in either the return period or the quantile sense, is uniquely defined by equation (3.12) with $C = C_Q$ or C_T respectively.

In the case where no proper contour exists we will need alternative methods for constructing a valid contour. One example of a possible construction is the following, here $x \in \mathbb{R}^d$ is some suitable centre point, ideally such that $C(u) - \langle u, x \rangle > 0$ for all $u \in S^{d-1}$, around which the contour is drawn.

$$\mathcal{B} = \text{cl} \left(\text{conv} \left(\{x + u(C(u) - \langle u, x \rangle)^+ : u \in S^{d-1}\} \right) \right), \quad (3.13)$$

where $(\cdot)^+$ equals $\max(\cdot, 0)$, $\text{conv}(\cdot)$ denotes the convex hull and $\text{cl}(\cdot)$ is the closure.

Proposition 3.10. *Fix some $t_s \in (0, \infty)$, $q_s \in (0, 1)$ such that $C_Q(u)$ is well defined for all $u \in S^{d-1}$ and bounded from above. Let \mathcal{B} be constructed as in equation (3.13) with $C = C_Q$, we then have that $\partial\mathcal{B}$ is a valid contour in the quantile sense.*

Similarly, if C_T is defined and bounded above for some $t_r \in (0, \infty)$ and $\hat{\mathcal{B}}$ is constructed as in (3.13) with $C = C_T$, we then have that $\partial\hat{\mathcal{B}}$ is a valid contour in the return period sense.

Proof. Since, by definition, $x + u(C_Q(u) - \langle u, x \rangle)^+ \in \mathcal{B}$ we have

$$B(\mathcal{B}, u) = \sup\{\langle u, v \rangle : v \in \mathcal{B}\} \geq \langle u, x + u(C_Q(u) - \langle u, x \rangle) \rangle = C_Q(u),$$

for any $u \in S^{d-1}$. Lastly, \mathcal{B} is closed and convex by definition, and since C_Q is bounded from above we have that $(C_Q(u) - \langle u, x \rangle)^+$ is bounded. As a consequence, \mathcal{B} is compact, making $\partial\mathcal{B}$ valid in the quantile sense. An identical argument shows that $\partial\widehat{\mathcal{B}}$ is valid in the return period sense. \square

To ensure that this construction is always feasible we have the following result, which ensures that C_Q and C_T are indeed bounded, thereby guaranteeing the existence of valid contours.

Lemma 3.11. *Fix some $t_r, t_s \in (0, \infty)$, $q_s \in (0, 1)$ such that C_T is well defined and assume that (3.10) holds. We then have that C_Q and C_T are bounded from above on S^{d-1} .*

Proof. Firstly, by Theorem 3.4, we have that C_Q is defined and finite for any $u \in S^{d-1}$. Furthermore, if we define $\phi_t^\infty = \sup_{s \in [0, t]} \|V_s\|$ we may note that (3.10) implies $\mathbb{P}(\phi_t^\infty = \infty) = 0$ for any $t \in (0, \infty)$.

As a consequence we may pick some $b \in \mathbb{R}$ such that $\mathbb{P}(\phi_{t_s}^\infty < b) > q_s$ and compute

$$\mathbb{P}(\tau_{\Pi^+(u, b)} > t_s) \geq \mathbb{P}(\phi_{t_s}^\infty < b) > q_s.$$

Due to this we see that $C_Q(u) < b$ for all $u \in S^{d-1}$.

Similarly, we may pick $b' \in \mathbb{R}$ such that $\mathbb{P}(\phi_{2t_r}^\infty < b') > 0.5$ which further implies

$$\mathbb{E}[\tau_{\Pi^+(u, b')}] \geq \mathbb{E}[\tau_{b' S^{d-1}}] \geq 2t_r \mathbb{P}(\tau_{b' S^{d-1}} > 2t_r) \geq 2t_r \mathbb{P}(\phi_{2t_r}^\infty < b') > t_r.$$

This implies $C_T(u) < b'$ for all $u \in S^{d-1}$. \square

With this result we can guarantee the existence of valid contours. However, other construction methods also exist. In [5], the authors consider a scenario where C_e could produce a proper contour, but due to estimation errors, the approximated C_e fails to do so. To address this issue, they propose constructing an inflated contour using (3.12) based on $C_e + c$ for some appropriate $c \in \mathbb{R}$. In a more general case where C_e does not admit a proper contour, as presented in [2], an invalid contour is constructed using (3.12), followed by an extension procedure that guarantees a valid construction in the limit. For both cases it is assumed that C_e is bounded, and hence Lemma 3.11 ensures that these methods can still be applied in our setting.

With the existence and construction of contours settled we can move on to some examples. The goal of these are to show the ways the presented methods differ from the existing framework presented in e.g. [6]. The first main difference is the ability to consider a continuous-time framework which more accurately captures the dynamics of V in between the discrete points at which it is measured. Secondly we can also allow non-stationary behaviour which allows the inclusion of effects like climate change as a part of the model of V .

4. THEORETICAL EXAMPLE

We will in this section aim to define a proper contour in the return period sense with a target return period of t_r under the assumption that V follows the continuous dynamics described below. Once this is done we will compare our exact method

with an i.i.d. method to highlight the differences. In analysing these models we also discuss when i.i.d. methods produce conservative estimates. Additionally, we provide a simple heuristic for when this is likely to be the case. It is also worth mentioning that a similar case was studied in [9]. Here several types of contours were compared for both continuous and discrete models of the underlying environmental factors based on several different procedures.

We here consider the case where $V_t \in \mathbb{R}^1$ is defined by

$$V_t = \sqrt{2\theta} \int_{-\infty}^t e^{-\theta(t-s)} dW_s,$$

where W is standard Brownian motion and $\theta \in \mathbb{R}$, $\theta > 0$. This makes V a standardised Ornstein-Uhlenbeck process which serves as a continuous interpolation of an AR(1) discrete-time process. Note that V is standardised to ensure a mean of 0 and variance 1, which implies V_t standard normally distributed for any t .

Since $-V$ satisfies $-V_t = \sqrt{2\theta} \int_{-\infty}^t e^{-\theta(t-s)} d(-W)_s$, we see that $-V$ is also an Ornstein-Uhlenbeck process with the same parameters and thus equal in law to V . As such we know that C_T is constant on $S^0 = \{-1, 1\}$. In fact, if we considered a d -dimensional Ornstein-Uhlenbeck process, C_T would still be constant and $\partial\mathcal{B}$ would equal a $d-1$ -sphere with a radius given by the same value of C_T as our 1-dimensional case.

In computing C_T we again consider $\mathcal{T}_u(b) = \mathbb{E}[\tau_{\Pi^+(u,b)}]$. Under the assumption that $V_0 = 0$ we have an explicit representation of $\mathcal{T}_u(\cdot)$, independent of u , given in e.g. [11] as

$$\mathcal{T}_u(b) = \frac{1}{2\theta} \sum_{i=1}^{\infty} \frac{(\sqrt{2}b)^i}{i!} \Gamma\left(\frac{i}{2}\right),$$

where Γ is the gamma function. One can also show the more convenient alternative representation of

$$\mathcal{T}_u(b) = \frac{\sqrt{\pi}}{\theta\sqrt{2}} \int_0^b \left(1 + \operatorname{erf}\left(\frac{t}{\sqrt{2}}\right)\right) e^{t^2/2} dt,$$

where erf denotes the error function. By inverting $\mathcal{T}_u(\cdot)$ we can easily compute C_T numerically and the resulting contour would, due to C_T being constant, be the two points given by $\partial\mathcal{B} = \{\pm\mathcal{T}_u^{-1}(t_r)\}$.

This gives us an explicit representation of the optimal contour. However, as an alternative we could consider a discrete model for V . We define $W = \{W_n\}_{n=0}^{\infty}$ as an independent sequence of standard normally distributed random variables. Further define \bar{V} by $\bar{V}_t = W_{\lfloor t/\Delta t \rfloor}$, for some $\Delta t > 0$ and note that V_t and \bar{V}_t are equal in law for any $t \in \mathbb{R}$. As such we consider \bar{V} as an alternative model of V .

If we were to apply the i.i.d. method presented in e.g. [6] we could compute C_T based on \bar{V} . We know that this is equivalent to considering C_e with an exceedance probability of $p_e = \Delta t/t_r$, which means that for all $u \in S^0$ we would have

$$C_e(u) = \Phi^{-1}\left(1 - \frac{\Delta t}{t_r}\right),$$

where Φ is the cumulative distribution function of a standard normal random variable.

With these two models we can compare how the resulting contours differ. Since both models provide perfectly circular contours (insofar as S^0 can be referred to as *circular*) we can instead compare the radii. To compute exact numbers we want realistic values for θ and Δt , which will be chosen based on a time series, $\{H_n\}_{n \in \mathbb{N}}$, of significant wave heights. The details of this dataset will be given in Section 5.

In order to choose our parameters we first pick $\Delta t = 3$ hours and compute the three hour autocorrelation (AC_3) of the standardized data $(H - \mu_H)/\sigma_H$. Here μ_H and σ_H are the empirical mean and standard deviation, respectively, of the time series $\{H_n\}_{n \in \mathbb{N}}$. By noting that the three-hour autocorrelation of an Ornstein-Uhlenbeck process satisfies $\theta = -\log(AC_3)/\Delta t$ we get $\theta = 0.016$.

The resulting radius curve based on the true model of V , labelled *OU Method*, and the curve based on \bar{V} , labelled *IID Method*, are plotted in Figure 1.

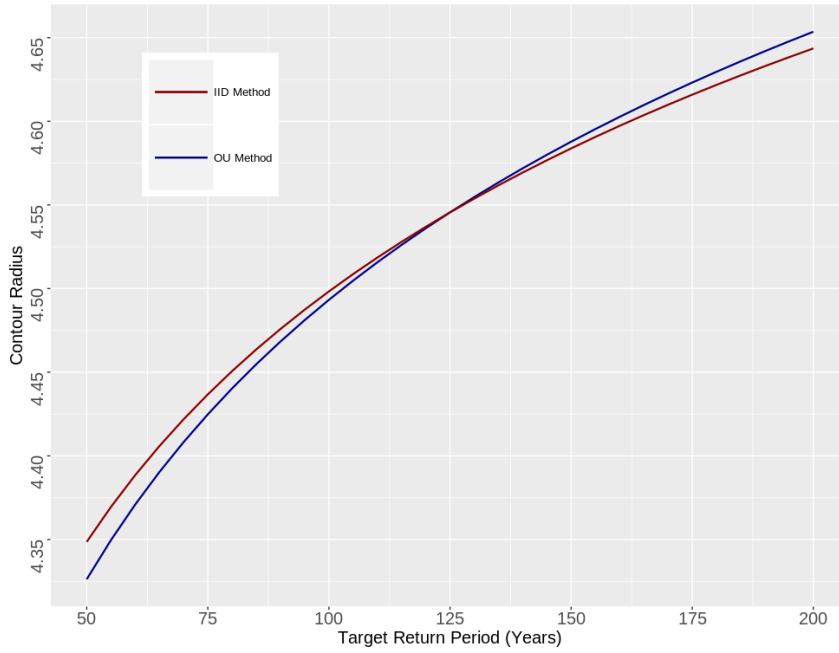


FIGURE 1. Comparison of contour radii for different methods

The differences are quite small, but there is still a noticeable distinction between the two methods. As we see the i.i.d. method produces larger and more conservative contours for low values of t_s , but crosses below for sufficiently large return periods. One can even find an approximation of when the two lines cross by noting that this point occurs when the radius, R , of the contour satisfies

$$\frac{\Delta t}{1 - \Phi(R)} = \mathcal{T}_u(R). \quad (4.1)$$

It can further be shown, by taking specific asymptotic expansions, that for high values of R we have the following approximations

$$\frac{\Delta t}{1 - \Phi(R)} \approx \Delta t \sqrt{2\pi} R e^{R^2/2}, \quad \mathcal{T}_u(R) \approx \frac{\sqrt{2\pi} e^{R^2/2}}{\theta R}.$$

Applying these to both sides of (4.1) then yields

$$\Delta t \sqrt{2\pi} R e^{R^2/2} \approx \frac{\sqrt{2\pi} e^{R^2/2}}{\theta R},$$

as long as the point where the lines cross occur for sufficiently high values of R . Simplifying this expression we get the approximate identity $\theta \Delta t R^2 = 1$, which means we can compute the return period for which this point occurs, here denoted t_r^* , by

$$t_r^* \approx \sqrt{\frac{2\pi \Delta t}{\theta}} e^{\frac{1}{2\theta \Delta t}}. \quad (4.2)$$

For our specific parameters our approximation yields $t_r^* \approx 130$ years.

By analysing (4.2) we can supplement the more heuristic reasons why these different models yield different contours.

Using \bar{V} ignores the autocorrelation, allowing the process to vary more wildly, usually producing larger contours. As such it is often considered as a conservative estimate. This effect is magnified when Δt is low which corresponds to the limit $\lim_{\Delta t \rightarrow 0} t_r^* = \infty$.

However, we see from this experiment that situations exist where this method can underestimate the risk due to not considering continuous time. Since the true model of V is continuous it has the possibility of hitting boundaries in-between the discrete points. Indeed, if we take an example of a ship on the sea, it could very well be that the ship can sustain the conditions of two time-points 3 hours apart while still capsizing at some moment in between. This effect is reflected by $\partial t_r^* / \partial \theta < 0$ which implies that increasing θ shrinks the domain where the method based on \bar{V} is conservative. Indeed, a high θ increases the volatility of V , thus improving the chances of the process exceeding a fixed boundary at times in-between the points of $\{n\Delta t, n \in \mathbb{N}\}$.

It is important to remark that these results are heavily reliant on \bar{V}_t equalling V_t in distribution. If we instead defined W_n to equal, in distribution, the maximal value of V_t in the period $[n\Delta t, (n+1)\Delta t]$ then we would no longer see this effect.

However, if the distribution of V_t 's maximum value over a 3-hour period was computed using e.g. the maximum of hourly point values, the effect would persist. Using 3-hour maxima affects the upper and lower point of $\partial \mathcal{B}$ differently, but if we were to consider the highest value of \mathcal{B} then the method of W based on 3-hour maxima will agree with the true value for

$$t_r^* \approx \sqrt{\frac{2\pi \Delta t}{3\theta}} e^{\frac{3}{2\theta \Delta t}}.$$

Given this we see that the discrete method can give non-conservative estimates when approximating the maxima with discrete point values for $t_r > t_r^*$.

When choosing between i.i.d. discrete-time and continuous-time models for the purposes of computing environmental contours it is possible to use these results as rule of thumb. The models used in this example can easily be calibrated to any time series, possibly with some transformation of the data to account for non-Gaussian tails, which allows us to compute the crossing point from (4.2). If the target return period is below this value then this example provides a heuristic for believing that models based on i.i.d. sequences are indeed conservative estimates.

5. EMPIRICAL EXAMPLE

The data considered for this example will consist of ERA5 reanalysis data [4]. We will use hourly data for significant wave height and wave periods from 65°N, 0°W over the period 1959-2021. While the calibration will use the full resolution of one hour, we will use a three-hour time step for the purposes of simulation and computation.

Our primary goal is here to compute an empirical proper contour in the quantile sense for a survival time of $t_s = 50$ years and a survival probability of $q_s = e^{-1} \approx 37\%$. In doing so we will also present a specific algorithm for generating such contours which is carried out in three steps:

- The distribution of V_t is estimated for all relevant values of t .
- Paths of V are simulated by using sequences of independent (but not necessarily identically distributed) random variables.
- These paths are used to compute samples of $\phi_{t_s}^u$ which allows the computation of C_T by Lemma 3.3.

Note that a survival probability of e^{-1} is chosen to correspond with a 50-year return period if τ had an exponential density. Due to the presence of a trend we do not have this distribution, but it will still serve as an easy, although rough, point of comparison.

5.1. Calibration of Distributions. We here have $V \in \mathbb{R}^2$ with $V_t = (P_t, H_t)$ where P and H denotes the wave period and significant wave height respectively. Following [6], [5], and [14] we model H using a 3-parameter Weibull distribution and P with a conditional log-normal distribution. However, due to the presence of long-term trends discussed in e.g. [15], [14], and [8] we will model V as non-stationary to take both this trend, as well as seasonality, into account.

We assume that $H_t \sim W(\lambda_t, k_t, \theta)$, i.e. a 3-parameter Weibull distribution with scale λ_t , shape k_t , and location θ . Here λ is taken to be on the form $\lambda_t = (c_1 + c_2 t)l_t$, furthermore, l and k are assumed periodic with a period of one year.

As for the wave period we assume that $(\log(P_t) | H_t = h) \sim \mathcal{N}(\mu(t, h), \sigma^2(t, h))$, i.e. a conditional normal distribution with mean $\mu(t, h)$ and variance $\sigma^2(t, h)$. Here μ and σ are assumed to be on the form $\mu(t, h) = m(t) + f_\mu(h)$ and $\sigma(t, h) = s(t)f_\sigma(h)$ where m and s are periodic with a period of one year.

In order to perform our calibration procedure we will first remark that if $H_t \sim W(\lambda_t, k_t, \theta)$, we then have for any $\lambda'_t, k'_t \in \mathbb{R}$ that

$$\frac{(H_t - \theta)}{\lambda'_t} \sim W\left(\frac{\lambda_t}{\lambda'_t}, k_t, 0\right), \quad (H_t - \theta)^{k'_t} \sim W\left(\lambda_t^{k'_t}, \frac{k_t}{k'_t}, 0\right).$$

To estimate (λ_t, k_t, θ) for H we then do the following.

- θ is estimated by the minimal measured value (rounded down to 2 significant digits to avoid numerical issues).
- The linear trend parameters, (c_1, c_2) , are estimated by linear regression on $H - \theta$.
- k_t is estimated by inverting the equality

$$\frac{\Gamma(1 + 1/k_t)^2}{\Gamma(1 + 2/k_t)} = \frac{\mathbb{E}[H_t - \theta]^2}{\mathbb{E}[(H_t - \theta)^2]},$$

where the expectations are computed by smoothing spline regression of $H - \theta$.

We then normalise k by defining $k'_t = k_t / \int_0^1 k_t dt$ so the average value of k' equals 1. This is done to avoid numerical issues from taking high powers.

- For calibration of l we note that

$$\mathbb{E}\left[\frac{(H_t - \theta_t)^{k'_t}}{(c_1 + c_2 t)^{k'_t}}\right] = l_t^{k'_t} \Gamma\left(1 + \frac{k'_t}{k'_t}\right).$$

We can then fit $l_t^{k'_t}$ by a smoothing spline regression of

$$\frac{(H_t - \theta_t)^{k'_t}}{(c_1 + c_2 t)^{k'_t} \Gamma(1 + \frac{k'_t}{k'_t})}.$$

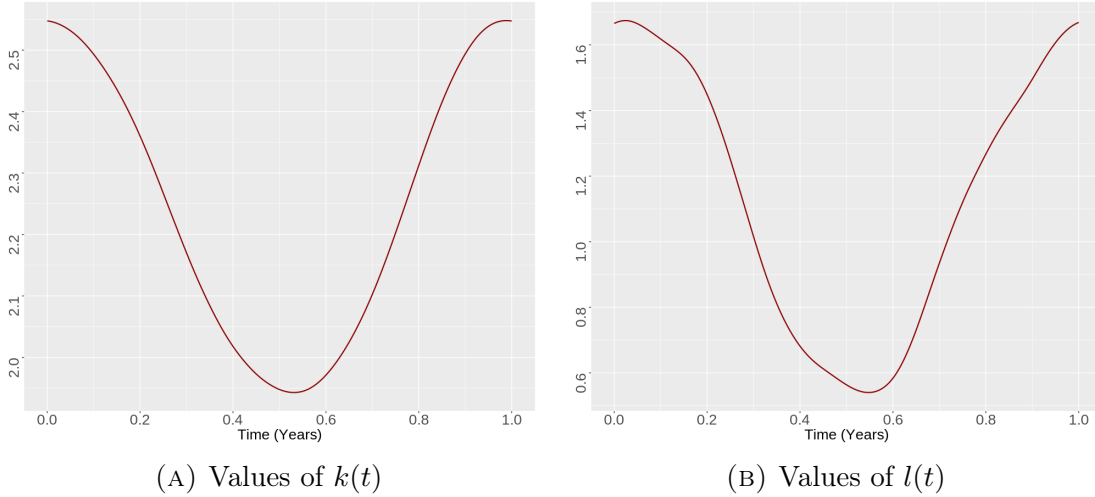


FIGURE 2. Non-parametric functions for H

θ	c_1	c_2
0.37 m	2.5 m	4.0e-3 m/y

TABLE 1. Parameters for H

The resulting parameters are given in Table 1 and Figure 2. Note that the parameters in Table 1 are given in meters (m) and meters per year (m/y), the functions in Figure 2 are dimensionless. Furthermore, we consider $t = 0$ to occur at the end of the dataset, i.e. the beginning of 2022.

As for P we do the following:

- We first estimate $\mu(t, h)$ by $\mathbb{E}[\log(P_t)|H_t] = \mu(t, H_t) = m(t) + f_\mu(H_t)$. With this we can fit smoothing splines for m and f_μ by generalized additive model calibration.
- Similarly, $\sigma(t, h) = s(t)f_\sigma(h)$ can be computed by

$$\mathbb{E}[\log(\log(P_t) - \mu(t, H_t))^2] = L + \log(s^2(t)) + \log(f_\sigma^2(H_t)),$$

where L is the log-moment of a chi-squared random variable with 1 degree of freedom. This allows us to fit smoothing splines for $\log(f_\sigma^2(h))$ and $\log(s^2(t))$ by a weighted generalized additive model calibration. Finally, to counteract issues arising from log-scale calibration, s is scaled to ensure that $(\log(P_t) - \mu(t, H_t)) / \sigma(t, H_t)$ has a variance of 1.

The resulting functions are given in Figure 3.

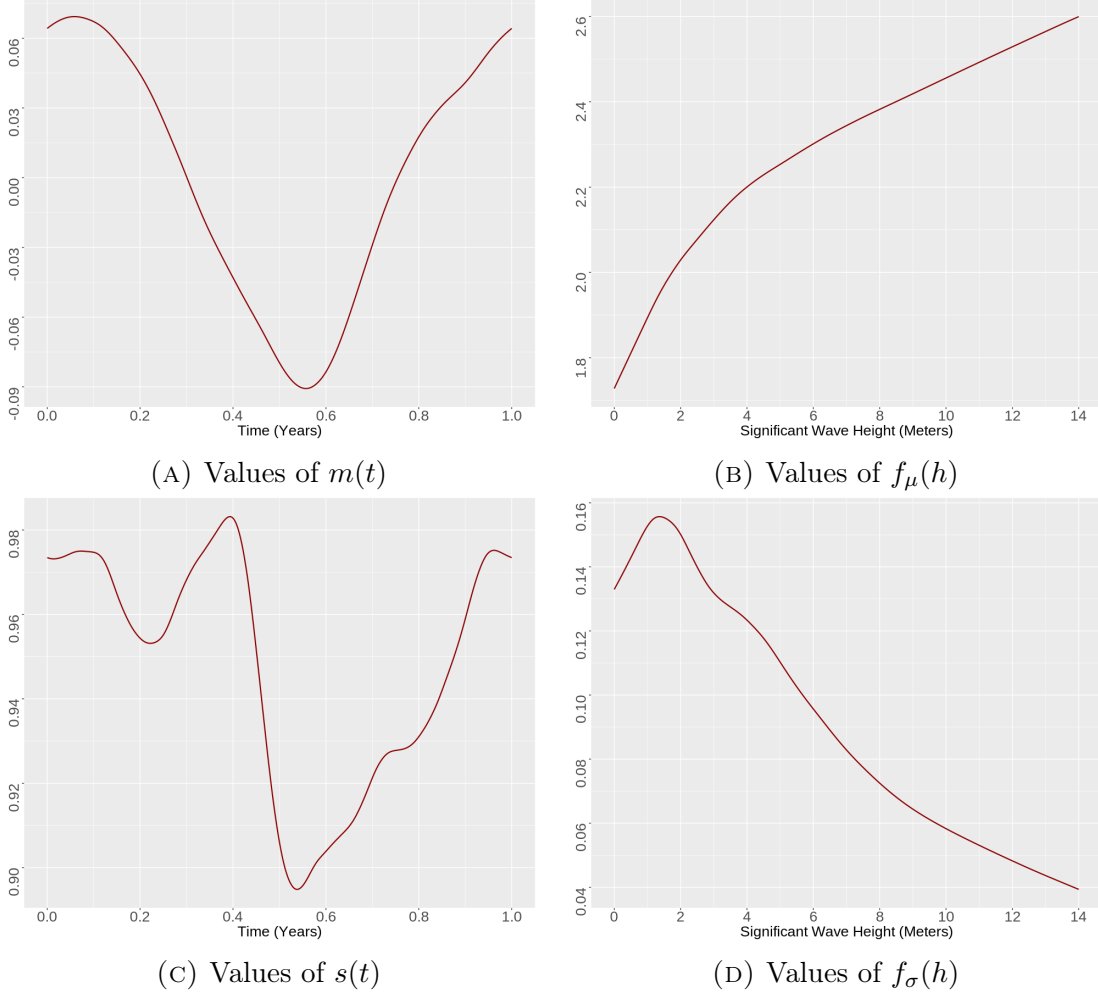
5.2. Simulation. With the d -dimensional marginal distributions of V determined we can move on to the computation of C_Q . Similarly to the previous example we define $\{W_n\}_{n=0}^\infty$ as a sequence of independent random variables such that $W_n = V_{n\Delta t}$ in distribution for $\Delta t = 3$ hours. This again lets us model V_t by $\bar{V}_t = W_{\lfloor t/\Delta t \rfloor}$.

Remark 5.1. Recall that if V was modelled by an i.i.d. sequence then our choice of (t_s, q_s) produces the same contours as a contour in the return period sense with a target return period of 50 years. Based on this equivalent return period we may consider our rule of thumb presented in the theoretical example. The rule states that an i.i.d. Gaussian method produces more conservative estimates than a continuous-time Ornstein-Uhlenbeck model for any target return period lower than 130 years. Our model for H is neither Gaussian nor stationary, but since it is based on independent samples of a time-varying distribution we have reason to suspect that our chosen modelling approach should be more conservative than a more complicated continuous one.

With this model we can easily simulate paths of \bar{V} over the next 50 years. Based on these simulations we obtain samples of $\phi_{t_s}^u$ for 180 uniformly spaced unit vectors in S^1 . By considering the lower q_s quantile of $\phi_{t_s}^u$ for a fixed $u \in S^1$ we obtain $C(u)$ by $q_s = \mathbb{P}(\tau_{\Pi^+(u, C(u))} > t_s) = \mathbb{P}(\phi_{t_s}^u \leq C(u))$.

In existing literature, such as [6] and [14], the inclusion of climatic trends is accomplished by considering a stationary distribution with parameters modified to reflect the observed trend. In order to study the effects of replacing the trend by adjusting parameters we will examine three cases by fixing the trend at either the beginning or end of our 50-year period.

- Case 1: $\lambda_t = (c_1 + c_2 * 50y)l_t$, which represents wave-states based on the trend 50 years after 2022.

FIGURE 3. Non-parametric functions for P

- Case 2: $\lambda_t = (c_1 + c_2 * t)l_t$, which represents the estimated true wave-states distributions.
- Case 3: $\lambda_t = c_1 l_t$, which represents wave-states based on the trend at the beginning of 2022.

Note that we here still include the seasonal effects. This is done to avoid using several calibration methods which could create artificial differences between the cases unrelated to the trend. However, despite seasonality, we would still expect case 1 and 3 to properly represent stationary alternatives to our method.

As we see there is a notable difference, though largely for angles corresponding almost purely with the significant wave height. This demonstrates that including trends is important to avoid underestimation of risk, such as in case 3. However, by including the trend as a non-constant effect, as in case 2, we can still safely reduce the resulting contour relative to case 1, where the highest trend value is applied to the entire period. Specifically, using the conservative estimate of case 1 still overestimates the risk significantly, with a maximal difference in C_T of 0.41. Since

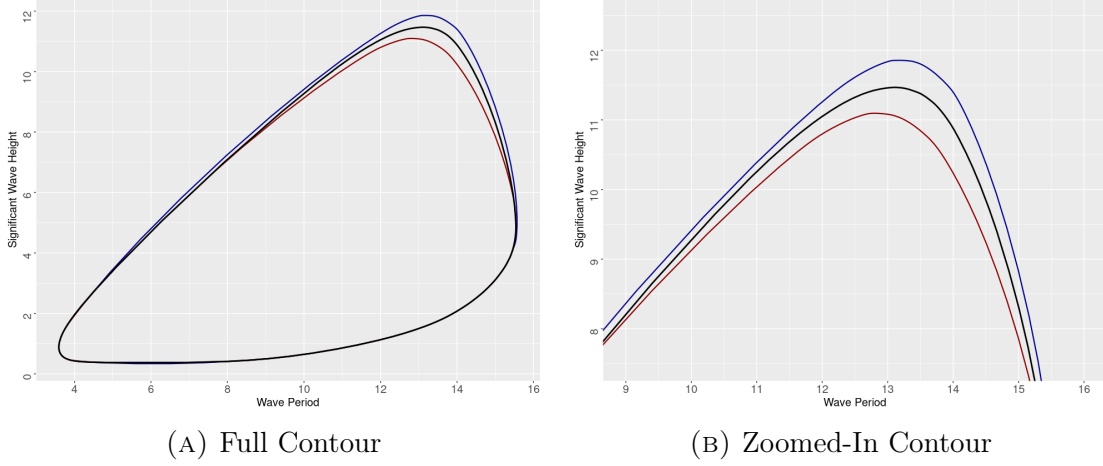


FIGURE 4. Environmental contours for case 1 (blue), case 2 (black), and case 3 (red)

the modelling of V by an i.i.d. process is inherently on the safe side we may be overly cautious by choosing a method which makes further conservative approximations.

6. SUMMARY AND CONCLUSIONS

This paper has rigorously defined and established minimal conditions for existence of environmental contours based on general stochastic processes. These definitions have several advantages over conventional constructions. Chiefly, the ability to properly include climate trends, but also the capability of including seasonality and autodependence.

One weakness of this approach, however, is the loss of efficient computational methods such as importance sampling which was considered in [5] for contours in the exceedance probability sense. A key problem here is the need to simulate paths of distributions rather than just quantiles of a single density. Despite this there is still room for further research when it comes to efficient or otherwise useful numerical methods, which could help remedy this issue. Other extensions, such as buffering, introduced in [1], can be readily extended to our setting, but may require restricting the model choice to those based on sequences of independent random variables.

Furthermore, the presented methods have also been compared to conventional techniques, and although some differences were minor there are still significant disparities. In particular, we have demonstrated that these methods can avoid the underestimation of risk coming from trends without the use of excessively conservative strategies. Finally, as part of these examples, we have also presented a strategy for computing these contours based on Monte-Carlo simulation. As such, the approaches considered are presented as an alternative method for the construction of environmental contours.

DECLARATION OF COMPETING INTEREST

The author declares that there is no known competing financial interest or personal relationship that could have appeared to influence the work reported in this paper

ACKNOWLEDGEMENTS

The author acknowledges financial support by the Research Council of Norway under the SCROLLER project, project number 299897.

REFERENCES

- [1] DAHL, K. R. ; HUSEBY, A. B.: Buffered environmental contours. In: *arXiv preprint arXiv:1903.12067* (2019)
- [2] HAFVER, A. ; AGRELL, C. ; VANEM, E. : Environmental contours as Voronoi cells. In: *Extremes* 25 (2022), Nr. 3, S. 451–486
- [3] HASSELSTEINER, A. F. ; COE, R. G. ; MANUEL, L. ; CHAI, W. ; LEIRA, B. ; CLARINDO, G. ; SOARES, C. G. ; HANNESDÓTTIR, Á. ; DIMITROV, N. ; SANDER, A. u. a.: A benchmarking exercise for environmental contours. In: *Ocean Engineering* 236 (2021), S. 109504
- [4] HERBACH, H. ; BELL, B. ; BERRISFORD, P. ; BIAVATI, G. ; HORÁNYI, A. ; MUÑOZ SABATER, J. ; NICOLAS, J. ; PEUBEY, C. ; RADU, R. ; ROZUM, I. ; SCHEPERS, D. ; SIMMONS, A. ; SOCI, C. ; DEE, D. ; THÉPAUT, J.-N. : ERA5 hourly data on single levels from 1959 to present. <http://dx.doi.org/10.24381/cds.adbb2d47>
- [5] HUSEBY, A. B. ; VANEM, E. ; AGRELL, C. ; HAFVER, A. : Convex environmental contours. In: *Ocean Engineering* 235 (2021), S. 109366
- [6] HUSEBY, A. B. ; VANEM, E. ; NATVIG, B. : A new approach to environmental contours for ocean engineering applications based on direct Monte Carlo simulations. In: *Ocean Engineering* 60 (2013), S. 124–135
- [7] HUSEBY, A. B. ; VANEM, E. ; NATVIG, B. : Alternative environmental contours for structural reliability analysis. In: *Structural Safety* 54 (2015), S. 32–45
- [8] KUSHNIR, Y. ; CARDONE, V. ; GREENWOOD, J. ; CANE, M. : The recent increase in North Atlantic wave heights. In: *Journal of Climate* 10 (1997), Nr. 8, S. 2107–2113
- [9] LEIRA, B. J.: A comparison of stochastic process models for definition of design contours. In: *Structural Safety* 30 (2008), Nr. 6, S. 493–505
- [10] MACKAY, E. ; HAUTECLOCQUE, G. de: Model-free environmental contours in higher dimensions. In: *Ocean Engineering* 273 (2023), S. 113959
- [11] RICCIARDI, L. M. ; SATO, S. : First-passage-time density and moments of the Ornstein-Uhlenbeck process. In: *Journal of Applied Probability* 25 (1988), Nr. 1, S. 43–57
- [12] ROSENBLATT, M. : Remarks on a multivariate transformation. In: *The annals of mathematical statistics* 23 (1952), Nr. 3, S. 470–472
- [13] ROSS, E. ; ASTRUP, O. C. ; BITNER-GREGERSEN, E. ; BUNN, N. ; FELD, G. ; GOULDBY, B. ; HUSEBY, A. ; LIU, Y. ; RANDELL, D. ; VANEM, E. u. a.: On environmental contours for marine and coastal design. In: *Ocean Engineering* 195 (2020), S. 106194
- [14] VANEM, E. ; BITNER-GREGERSEN, E. M.: Stochastic modelling of long-term trends in the wave climate and its potential impact on ship structural loads. In: *Applied Ocean Research* 37 (2012), S. 235–248
- [15] VANEM, E. ; HUSEBY, A. B. ; NATVIG, B. : A Bayesian hierarchical spatio-temporal model for significant wave height in the North Atlantic. In: *Stochastic environmental research and risk assessment* 26 (2012), S. 609–632
- [16] WINTERSTEIN, S. R. ; UDE, T. C. ; CORNELL, C. A. ; BJERAGER, P. ; HAVER, S. : Environmental parameters for extreme response: Inverse FORM with omission factors. In: *Proceedings of the ICOSSAR-93, Innsbruck, Austria* (1993), S. 551–557